Submitted to ADVANCED MATERIALS
DOI: 10.1002/adma.((please add manuscript number))

Coplanar Asymmetrical Reduced Graphene Oxide-Titanium Electrodes for Polymer Photodetectors

By Shuping Pang, Shubin Yang, Xinliang Feng, and Klaus Müllen**

[*] Dr. S. Pang, Dr. S. Yang, Prof. X. Feng and Prof. K. Müllen
Max Planck Institute for Polymer Research, Ackermannweg 10, D-55128 Mainz (Germany)
E-mail: feng@mpip-mainz.mpg.de; muellen@mpip-mainz.mpg.de
Prof. X. Feng
School of Chemistry and Chemical Engineering, Shanghai Jiao Tong University, 800 Dongchuan Road, Shanghai 200240, China

[**] This work was financially supported by the Max Plank Society through the program ENERCHEM, DFG Priority Program SPP 1355, DFG MU 334/32-1, DFG Priority Program SPP 1459, and ESF Project GOSPEL (Ref Nr: 09-EuroGRAPHENE-FP-001), EU Project GENIUS and ERC grant on NANOGRAPH.

Keywords: Photodetector, photodiode, graphene, asymmetrical electrodes, plasma etching

Photodetectors, converting light signals into a voltage or current, have been widely used in imaging, spectroscopy, fiber-optic communications and time-gated distance measurements.[1-3] Recently, polymer photodetectors have become increasingly attractive for detection technologies due to their high optical absorption coefficient, flexibility, processability and potential for low cost fabrication.[1, 3-6]

In general, there are two different types of polymer photodetectors, namely photoconductors and photodiodes as presented in Figures 1(a) and (b).[3, 7] Typically, polymer photoconductors (Figure 1a) employ two identical coplanar electrodes sandwiching a semiconducting polymer layer.[3, 8, 9] Under illumination, the conductance of the semiconductor layer will increase due to the formation of photogenerated carriers.[3] The difference of the conductance of the polymer under light versus dark is thus proportional to the light intensity. However, large amounts of photogenerated electron-hole pairs can quickly recombine in the channel before they reach the electrodes. In this regards, a narrow channel length (several hundred nanometers) and a high operation voltage are required to efficiently dissociate electron-hole pairs and subsequently sweep them to the electrodes before their recombination.[10] The traditional fabrication methods for narrow electrode gaps strongly depend on the equipment, such as e-beam lithography and atomic force microscopy

nanolithography.[11-13] By applying standard e-beam lithographic techniques, the gaps can be down to a few tens of nanometers in width. The second type of polymer photodetectors is the photodiode, which is normally fabricated in a sandwich structure as illustrated in Figure 1(b) with two different electrodes of which at least one is transparent.[3, 14-16] In this structure, the distance between the two electrodes can be easily reduced to tens to hundreds of nanometers via controlling the thickness of the semiconducting layer. Most importantly, the electron-hole recombination time can be efficiently delayed in the sandwich structure because of the formation of a built-in potential between the two electrodes. However, the disadvantages of this device are the complicated processing and the light reflection and absorption at the transparent electrode.[3, 16-18]

In this communication, we present a novel and simple strategy for fabricating coplanar asymmetrical reduced graphene oxide (RGO)-titanium (Ti) electrodes (AGTEs), which can avoid the drawbacks of each type of photodetectors and fulfill the requirements of low light consumption and high photosensitivity (Figure 1c). RGO is selected as the hole transport electrode because of its suitable work function (4.75 eV)[19] and high carrier injection efficiency to organic materials, such as poly(3-hexylthiophene) (P3HT) and pentacene, which have been demonstrated in organic solar cells and field effect transistors (OFETs). The employment of RGO electrode can reduce the contact resistance between electrode and organic semiconductors.[19-25] As electron transport electrode, titanium is employed for its good chemical stability and suitable work function. The combination of oxygen plasma etching and evaporation allows the patterning of AGTEs with narrow channel length. As a result, polymer photodetectors for both P3HT and a blend of P3HT with phenyl-C61-butyric acid methyl ester (PCBM) offers an improved photosensitivity by using AGTEs compared with those constructed on symmetrical electrodes.

The fabrication of coplanar AGTEs is illustrated in Scheme 1. First, a graphene oxide (GO) dispersion was spin-coated on a SiO_2/Si substrate and then thermally annealed to render the GO film electrically conductive (Scheme 1a). To define the RGO patterns, aluminum patterns were thermally evaporated through a homemade mask with 1 mm × 2 mm rectangular holes (Figure S1a) on the 20 nm thick RGO film (Scheme 1b). Subsequently, the silicon/RGO/aluminum substrate was exposed to oxygen plasma to remove the RGO regions not covered by the aluminum. Long-time plasma etching could produce an undercut along the edges of the aluminum patterns (Scheme 1c). After 3 min of oxygen etching, a 40 nm thick titanium layer was evaporated through another homemade mask with a 1 mm × 7 mm rectangular hole (Figure S1b) on top of the aluminum patterns (Scheme 1d). Finally, the

RGO-Ti patterns arranged alternately on the silicon substrate were obtained after removing the pre-deposited sacrificial aluminum patterns.

The patterned coplanar AGTEs are characterized by means of optical microscopy (OM) and atomic force microscopy (AFM) as shown in Figure 2. Apparently, the RGO electrodes (white, ~ 1 mm × 2 mm rectangles) and titanium electrodes (yellow, ~ 1 mm × 1 mm squares) are alternately deposited on the SiO_2/Si substrate (Figure 2a). The sharp and regular contact edges are noticeable in the AFM image (Figure 2b). Therefore, the areas exposed to the oxygen plasma were completely etched away, while the areas protected by aluminum had survived during the processing. It was found that a channel length of ~ 500 nm between RGO and titanium electrodes was generated after 3 min of plasma etching. The corresponding height profile (Figure 2c) along the line in Figure 2(b) indicates the complete etching of the RGO contacts down to the underlying silicon substrate. The formation of the gap is due to the undercut of the RGO film under the aluminum patterns. The length of the undercut increases when extending the oxygen plasma etching time. When using 20 sccm oxygen flow, 300 W rf power, the oxygen plasma etching rate of the covered RGO film is ~ 14 nm/sec (Figure S2). The channel length can therefore be easily adjusted by controlling the oxygen plasma etching time. Additionally, this fabrication process will also allow the fabrication of different asymmetrical electrodes with various work functions, such as graphene/gold and graphene-silver. In view of the application as electrodes in polymer photodetectors, the electron collecting electrode should possess a work function lower than the energy level of the lowest unoccupied molecular orbital (LUMO) of the photoactive semiconductor. Ttitanium, with a work function of - 4.3 eV, was chosen as suitable material to collect electrons and block holes from the P3HT layer.[26]

To examine the feasibility of the as-fabricated coplanar AGTEs in polymer photodetectors, P3HT and a blend of P3HT with PCBM were used as photosensitive materials. Before the device fabrication, the substrate with the AGTEs was firstly treated with 1,1,1,3,3,3-hexamethyldisilazane (HMDS) to render the surface hydrophobic. Subsequently, P3HT or P3HT: PCBM (1:0.8) was spin coated on top of the modified AGTEs and then annealed at 120 ^{o}C for 10 min. The photodetectors were finally tested in a glove box under a light source with intensity of ~ 20 mW/cm^2.

Typical Current-Voltage (I-V) characteristics of P3HT photodetectors based on the AGTEs are shown in Figure 3(a). The I-V curve in the dark displays an obvious diode behavior. Under illumination, the I-V curve moves far away from the origin (0,0). Like a

micro photovoltaic cell, the AGTEs based photodetector shows an open circuit voltage (V_{oc}) of 0.12 V and a short circuit current (I_{sc}) of 0.98 nA (Figure 3a). The large difference of the currents in the dark and under illumination around the origin (0,0) allows the device to be run at very low bias voltage, offering the possibility of working at low energy consumption. Figure 3(b) reveals the on/off characteristics of the photodetector at 0 V bias. The current of the devices is rather low in the dark, whereas it jumps sharply by more than 3 orders of magnitude upon irradiation (~ 20 mW/cm^2), indicating a high photosensitivity. Further, switching the shielded light alternately on and off causes the current of the devices to exhibit two distinct steady states: the "low" current state in the dark and the "high" current state in the light as shown in Figure 3(b). Additionally, the on current of the photodetector measured with the light intensity of 10 mW/cm^2 at 0 V showed a value of 0.48 nA, which is almost half of that working under 20 mW/cm^2, indicating a linear trend with the light intensity.

In order to further improve the photosensitivity of the P3HT photodetector, PCBM can be introduced as electron acceptor material which can promote the dissociation efficiency of the excitons or hole-electron pairs respectively, at the interface of a P3HT:PCBM into free holes and electrons.[27-30] The performance of the P3HT:PCBM photodetector based on the as-fabricated AGTE is presented in Figure 3(c, d). The I–V characteristic under illumination (Figure 3c) also displays a typical photodiode character with the V_{oc} of 0.46 V and I_{sc} of 2.0 nA. Apparently, both the V_{oc} and the I_{sc} are higher than those of the above P3HT photodetectors due to a more efficient dissociation of the excitons into free electrons, resulting in a high photosensitivity when the light is switched on and off (Figure 3d).

To gain an in-depth understanding of the influence of asymmetrical electrodes on the performance of photodetectors, two reference devices based on symmetrical gold contacts with a channel length of 5 μm were investigated. As indicated in Figure 4(a, c), the diode properties could not be observed when P3HT and P3HT/PCBM were utilized as photosensitive materials, respectively. In this way, a high applied bias voltage was required in order to achieve efficient exciton dissociation. However, the applied bias voltage can also exert an influence on the background current. For instance, the I-V curves of P3HT photodetector performed at 0.4 V bias shows a small variation between the conditions in the dark and under light (Figure 4a). The photocurrent and the dark current are of the same order and the on/off ratio is calculated to be less than 2. Additionally, the current of the photodetector increases and decreases more slowly than that of the P3HT photodetector based on the AGTEs when the light is turned on and off (Figure 3b, 3d). This can be attributed to the inefficient dissociation of holes and electrons in P3HT under illumination.[10, 27] After

introducing the electron acceptor, PCBM, both the on/off ratio and the photoresponse time are improved as demonstrated in Figure 4(d). The on/off ratio of the P3HT:PCBM photodetector at 0.4 V is ~ 10, about 5 times higher than that of the pure P3HT photodetector (Figure 4b). However, the on/off characteristic is not reversible, with a decreasing on-current along with repeating on/off operation (Figure 4d).

Apparently, the photodetectors of P3HT and PCBM based on the as-fabricated coplanar AGTEs reveal an improved performance compared with that based on the symmetrical gold electrodes (Table S1).[10, 27] The improvement is attributed to a "built-in" potential, which is governed by the difference of the work functions between two electrodes.[17, 22, 31, 32] The energy band diagrams of the photoactive materials and the asymmetrical electrodes are illustrated in Figure 5(a), while the corresponding simplified energy band diagrams are shown in Figure 5(b). When the external circuit is shorted, the energy levels of the graphene and titanium electrodes are rectified to the same value and an internal "built-in" electrical field can be produced in the photoactive layer (Figure 5c). In this case, the photoinduced holes and electrons in the polymer layer can quickly move to the opposite electrodes, resulting in the improved photosensitivity. Additionally, the presence of a built-in potential is also beneficial for the low voltage operation, fulfilling the requirement of low energy consumption for the future photodetectors.

In summary, we have demonstrated the fabrication of coplanar asymmetrical graphene-titanium electrodes. The fabrication technology involving evaporation of protective layer and oxygen plasma etching is simple and suitable to pattern electrodes with narrow gaps of several hundreds of nanometers. The P3HT photodetectors based on the patterned graphene-titanium electrodes result in improved photosensitivity because of the narrow gap and the "built-in" potential originating from the different electrodes, which can efficiently dissociate the excitons into free holes and electrons and then quickly drive them to the opposite electrodes. The easy processing, high photosensitivity, high on/off ratio and low energy consumption lead to a promising potential of the coplanar asymmetrical electrodes in the field of photoelectric devices.

Experimental

Preparation of the asymmetrical RGO-Ti electrode: First, a GO dispersion prepared from natural graphite by the Hummers method was sonicated for 3 h and then spin-coated on a SiO_2/Si substrate. Then the GO film was thermally reduced at 1000 ^oC for 30 min with a heating rate of 1 ^oC/min. The conductivity of the RGO film is ~ 500 S/cm, which was

measured by a standard four point-probe system with a Keithley 2700 Multimeter (probe spacing: 0.635 mm, Rs=4.5324* V/I).. Subsequently, a 60 nm thick aluminum layer was thermally evaporated under vacuum on the RGO film through a home made mask with 1 mm × 2 mm rectangular holes. The substrate was then exposed in an oxygen plasma cleaner (Plasma System 200) for 3 min with a 20 sccm oxygen flow, 300 W rf power. Then a 40 nm thick titanium layer was evaporated on top of the aluminum patterns through another homemade mask with a 1 mm × 7 mm rectangular hole on the top of the aluminum patterns. Finally, the asymmetrical RGO-Ti electrodes were obtained after removing the aluminum by immersing the sample in a 5 % HNO_3 solution for 60 min.

Device fabrication and measurements: The chloroform solution of P3HT (5 mg/mL, 4002-E, Rieke Metals, Inc.) or a mixture of P3HT (5 mg/mL) and PCBM (4 mg/mL, Aldrich 684430) was spin-coated at 2000 rpm for 40 s on top of the asymmetrical RGO-Ti electrodes. The photodetectors were tested in a glove box under nitrogen atmosphere with a Keithley SCS 4200 semiconductor characterization system. The light of a Nikon microscopy (SMZ1000, ~ 20mW/cm^2) was directly used to switch on the photodiode.

Received: ((will be filled in by the editorial staff))
Revised: ((will be filled in by the editorial staff))
Published online: ((will be filled in by the editorial staff))

References

[1] X. Gong, M. H. Tong, Y. J. Xia, W. Z. Cai, J. S. Moon, Y. Cao, G. Yu, C. L. Shieh, B. Nilsson, A. J. Heeger, *Science* **2009**, *325*, 1665.
[2] G. Konstantatos, I. Howard, A. Fischer, S. Hoogland, J. Clifford, E. Klem, L. Levina, E. H. Sargent, *Nature* **2006**, *442*, 180.
[3] G. Konstantatos, E. H. Sargent, *Nat. Nanotechnol.* **2010**, *5*, 391.
[4] G. A. O'Brien, A. J. Quinn, D. A. Tanner, G. Redmond, *Adv. Mater.* **2006**, *18*, 2379.
[5] B. Pradhan, K. Setyowati, H. Y. Liu, D. H. Waldeck, J. Chen, *Nano Lett.* **2008**, *8*, 1142.
[6] S. Liu, J. M. Li, Q. Shen, Y. Cao, X. F. Guo, G. M. Zhang, C. Q. Teng, J. Zhang, Z. F. Liu, M. L. Steigerwald, D. S. Xu, C. Nuckolls, *Angew. Chem. Int. Ed.* **2009**, *48*, 4759.
[7] S. Wan, J. Guo, J. Kim, H. Ihee, D. L. Jiang, *Angew. Chem. Int. Ed.* **2009**, *48*, 5439.
[8] V. Sukhovatkin, S. Hinds, L. Brzozowski, E. H. Sargent, *Science* **2009**, *324*, 1542.
[9] H. Y. Chen, M. K. F. Lo, G. W. Yang, H. G. Monbouquette, Y. Yang, *Nat. Nanotechnol.* **2008**, *3*, 543.
[10] Y. Cao, S. Liu, Q. Shen, K. Yan, P. J. Li, J. Xu, D. P. Yu, M. L. Steigerwald, C. Nuckolls, Z. F. Liu, X. F. Guo, *Adv. Funct. Mater.* **2009**, *19*, 2743.
[11] T. Takahashi, T. Takenobu, J. Takeya, Y. Iwasa, *Adv. Funct. Mater.* **2007**, *17*, 1623.
[12] S. Cho, J. Yuen, J. Y. Kim, K. Lee, A. J. Heeger, *Appl. Phys. Lett.* **2007**, *90*, 063511.
[13] J. M. Mativetsky, A. Liscio, E. Treossi, E. Orgiu, A. Zanelli, P. Samori, V. Palermo, *J. Am. Chem. Soc.* **2011**, *133*, 14320.

[14] P. Peumans, V. Bulovic, S. R. Forrest, *Appl. Phys. Lett.* **2000**, *76*, 3855.
[15] T. Rauch, M. Boberl, S. F. Tedde, J. Furst, M. V. Kovalenko, G. N. Hesser, U. Lemmer, W. Heiss, O. Hayden, *Nat. Photonics* **2009**, *3*, 332.
[16] N. C. Greenham, X. G. Peng, A. P. Alivisatos, *Phys. Rev. B* **1996**, *54*, 17628.
[17] Y. H. Chang, C. M. Liu, Y. C. Tseng, C. Chen, C. C. Chen, H. E. Cheng, *Nanotechnology* **2010**, *21*, 225602.
[18] S. W. Clark, J. M. Harbold, F. W. Wise, *J. Phys. Chem. C* **2007**, *111*, 7302.
[19] A. Liscio, G. P. Veronese, E. Treossi, F. Suriano, F. Rossella, V. Bellani, R. Rizzoli, P. Samori, V. Palermo, *J. Mater. Chem.* **2011**, *21*, 2924.
[20] Q. Su, S. P. Pang, V. Alijani, C. Li, X. L. Feng, K. Mullen, *Adv. Mater.* **2009**, *21*, 3191.
[21] S. P. Pang, H. N. Tsao, X. L. Feng, K. Müllen, *Adv. Mater.* **2009**, *21*, 3488.
[22] M. Y. Liu, C. H. Chang, C. H. Chang, K. H. Tsai, J. S. Huang, C. Y. Chou, I. J. Wang, P. S. Wang, C. Y. Lee, C. H. Chao, C. L. Yeh, C. I. Wu, C. F. Lin, *Thin Solid Films* **2010**, *518*, 4964.
[23] U. J. Kim, H. Bin Son, E. H. Lee, J. M. Kim, S. C. Min, W. Park, *Appl. Phys. Lett.* **2010**, *97*, 032117.
[24] S. P. Pang, Y. Hernandez, X. L. Feng, K. Müllen, *Adv. Mater.* **2011**, *23*, 2779.
[25] Z. F. Liu, Q. Liu, Y. Huang, Y. F. Ma, S. G. Yin, X. Y. Zhang, W. Sun, Y. S. Chen, *Adv. Mater.* **2008**, *20*, 3924.
[26] S. Cho, K. Lee, A. J. Heeger, *Adv. Mater.* **2009**, *21*, 1941.
[27] H. F. Zhu, T. Li, Y. J. Zhang, H. L. Dong, J. S. D. Song, H. P. Zhao, Z. M. Wei, W. Xu, W. P. Hu, Z. S. Bo, *Adv. Mater.* **2010**, *22*, 1645.
[28] I. W. Hwang, D. Moses, A. J. Heeger, *J. Phys. Chem. C* **2008**, *112*, 4350.
[29] M. S. Arnold, J. D. Zimmerman, C. K. Renshaw, X. Xu, R. R. Lunt, C. M. Austin, S. R. Forrest, *Nano Lett.* **2009**, *9*, 3354.
[30] G. Yu, J. Wang, J. McElvain, A. J. Heeger, *Adv. Mater.* **1998**, *10*, 1431.
[31] B. Zimmermann, M. Glatthaar, M. Niggemann, M. Riede, A. Hinsch, *Thin Solid Films* **2005**, *493*, 170.
[32] T. Mueller, F. N. A. Xia, P. Avouris, *Nat. Photonics* **2010**, *4*, 297.

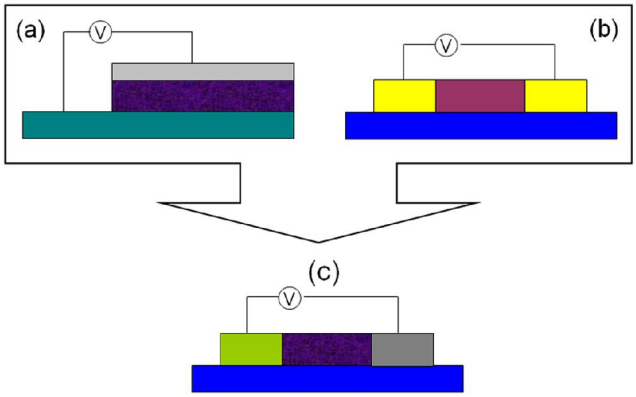

Figure 1. Structural models of (a) coplanar photoconductor with two symmetrical electrodes, (b) sandwich photodiode with two asymmetrical electrodes (one is transparent), (c) coplanar photodetector with two asymmetrical electrodes.

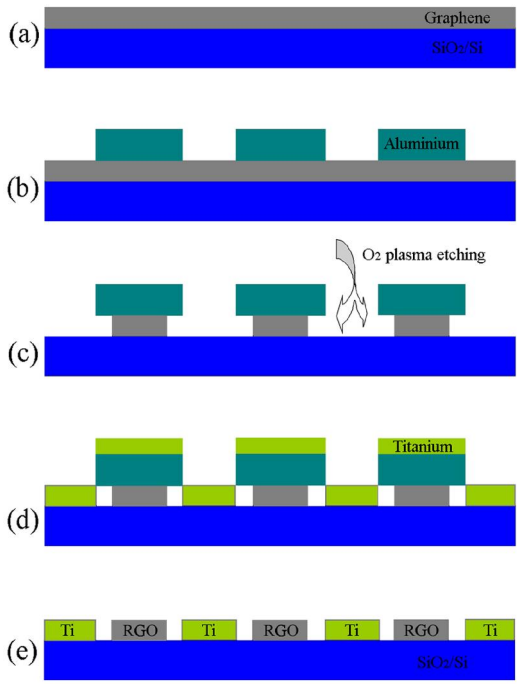

Scheme 1. Schematic illustration of the fabrication process of AGTEs. (a) A graphene film was produced by thermal reduction of a GO film. (b) Patterned aluminum was evaporated to serve as the sacrificial mask. (c) An undercut along the edges of the patterned aluminum patterns was formed via long-time oxygen plasma etching of the graphene film. (d) Titanium electrodes were evaporated directly on the etched film. (e) Patterned AGTEs were obtained after washing away the sacrificial aluminum layer.

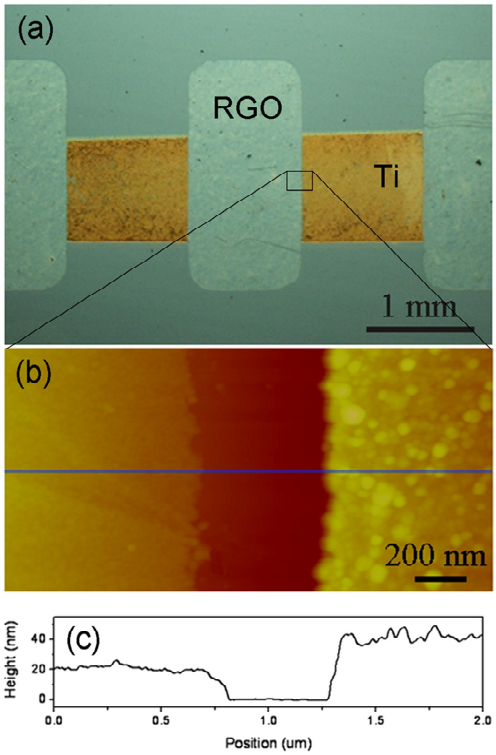

Figure 2. (a) OM image of AGTEs, white rectangles are RGO and yellow squares are Ti, respectively. (b) AFM image of the edge of the RGO-Ti electrodes, indicating a channel length of ~ 500 nm. (c) Height profile along the line in (b), showing a narrow channel etched down to the underlying SiO_2/Si substrate.

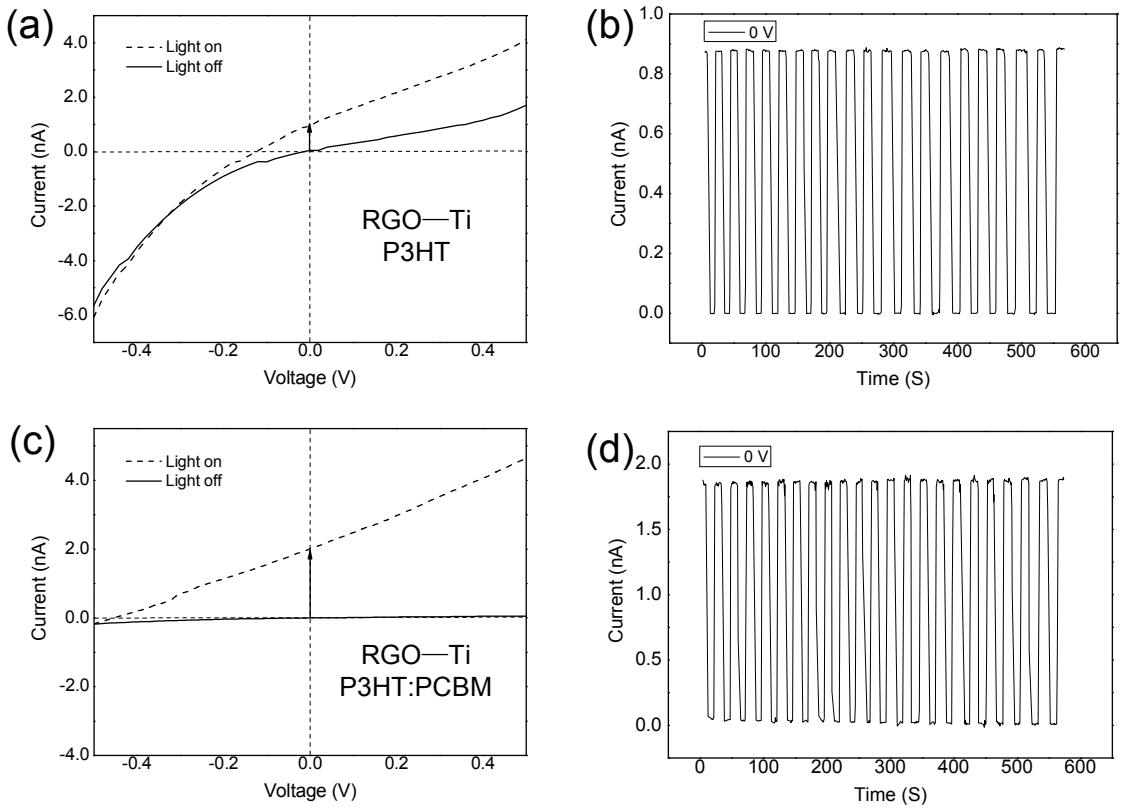

Figure 3. (a) I–V characteristics of the AGTEs based photodetector with P3HT as the photosensitive material. (b) The on/off characteristics of the P3HT photodetector at 0 V bias. (c) I–V characteristics of the AGTEs based photodetector with the blend of P3HT:PCBM as the photosensitive material. (d) The on/off characteristics of the P3HT:PCBM photodetector at 0 V bias.

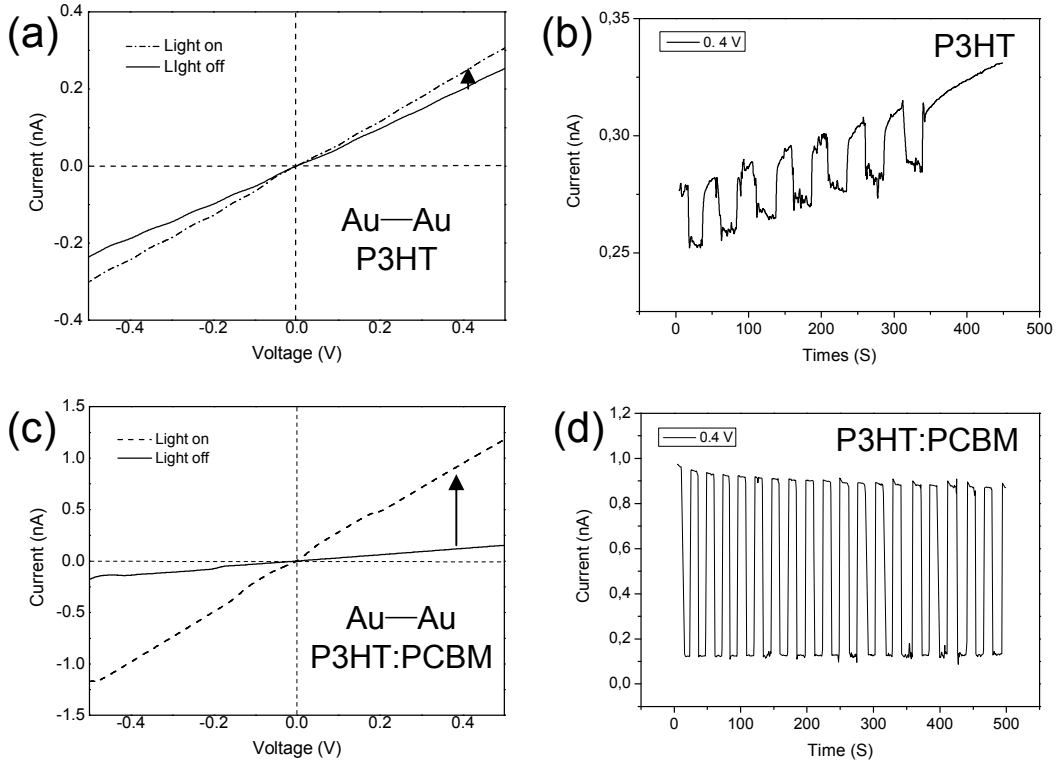

Figure 4. (a) I–V characteristics of the symmetrical gold electrode based photodetector with P3HT as the photosensitive material. (b) The on/off characteristics of the P3HT photodetector at 0.4 V. (c) I–V characteristics of the symmetrical gold electrodes based photodetector with the blend of P3HT:PCBM as photosensitive material. (d) The on/off characteristics of the P3HT:PCBM photodetector at 0.4 V.

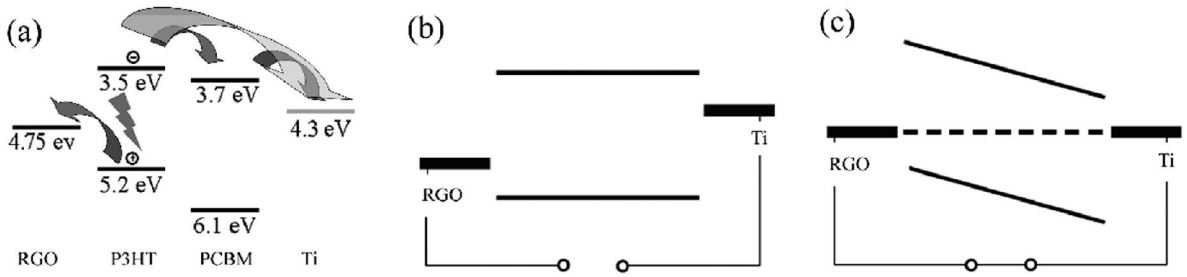

Figure 5. (a) A schematic representation of charge transfer and transport as an energy level diagram. (b-c) Simplified principles of device function for organic semiconducting layers between two metallic electrodes: (b) open circuit (flat band) condition, (c) short circuit condition.

The table of contents

A combination of oxygen plasma etching and evaporation process was developed to fabricate coplanar asymmetrical RGO-Ti electrodes with narrow gaps. The polymer poly(3-hexylthiophene) photodetectors based on the as-fabricated asymmetrical electrodes exhibit improved photosensitivity compared to that based on symmetrical electrodes, which is attributed to the narrow gaps and the "built-in" potential originated from the different work function of graphene and titanium electrodes. As a result, such feature of asymmetrical electrodes renders an efficient dissociation of the excitons to free holes and electrons which can be readily repelled to opposite electrodes. The easy processing, high photosensitivity, high on/off ratio and low energy consumption have revealed the promising potential of the coplanar asymmetrical electrodes in the field of photoelectric devices.

Keywords: Photodetector, photodiode, graphene, asymmetrical electrodes, plasma etching,

Shuping Pang, Shubin Yang, Xinliang Feng*, and Klaus Müllen*

Coplanar Asymmetrical Reduced Graphene Oxide-Titanium Electrodes for Polymer Photodetectors

ToC figure ((55 mm broad, 50 mm high, or 110 mm broad, 20 mm high))

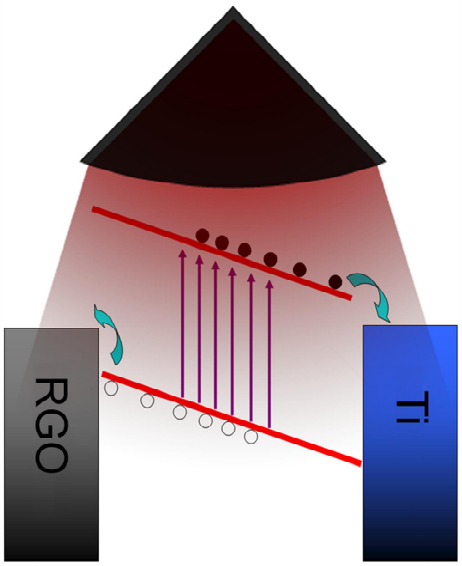

Submitted to ADVANCED MATERIALS

Supporting Information

Coplanar Asymmetrical Reduced Graphene Oxide-Titanium Electrodes for Polymer Photodetectors

Shuping Pang, Shubin Yang, Xinliang Feng*, and Klaus Müllen*

[*] Dr. S. Pang, Dr. S. Yang, Prof. X. Feng and Prof. K. Müllen
Max Planck Institute for Polymer Research, Ackermannweg 10, D-55128 Mainz (Germany)
E-mail: feng@mpip-mainz.mpg.de; muellen@mpip-mainz.mpg.de
Prof. X. Feng
School of Chemistry and Chemical Engineering, Shanghai Jiao Tong University, 800 Dongchuan Road, Shanghai 200240, China

E-mail: feng@mpip-mainz.mpg.de; muellen@mpip-mainz.mpg.de

Tel: +49-6131379151 Fax: +49-6131379350

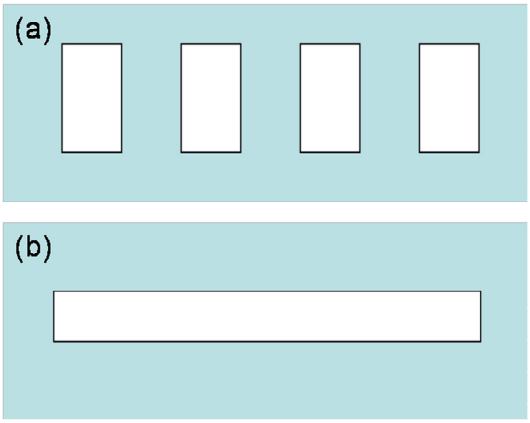

Figure S1. Home-made masks for pattern the asymmetrical graphene-titanium electrodes. The width of the white square is 1 mm.

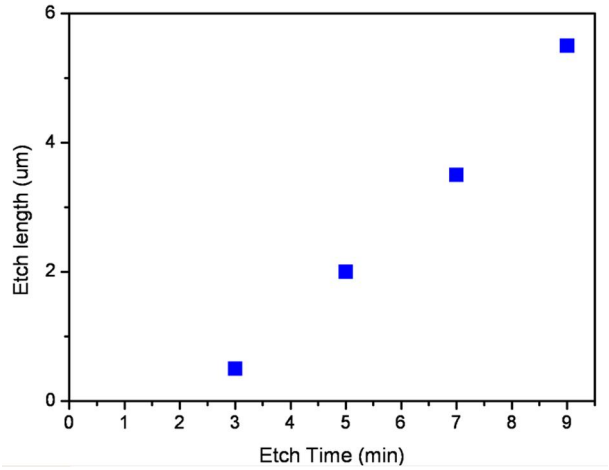

Figure S2. The rate of the oxygen etching of the RGO film. It was calculated that the lateral etching rate of graphene film under the aluminum is ~ 10 nm per second with 20 sccm O_2 flow, 300 W rf power. Thus, the channel length can be easily adjusted by controlling the plasma etching time. This fabrication strategy is therefore supposed to be a promising to pattern nanometer-sized gaps for nano-devices.

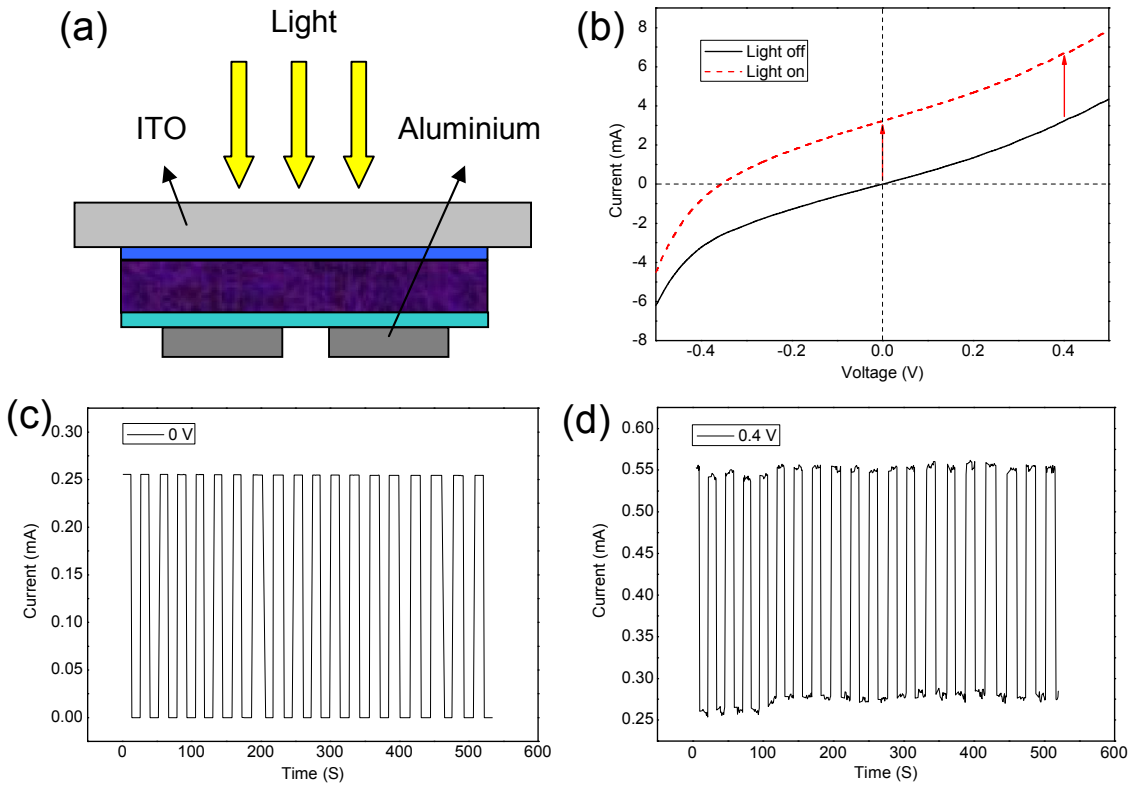

Figure S3. P3HT:PCBM photodetector based on a sandwich structure.

For comparison, a P3HT:PCBM photodetector based on a sandwich structure was fabricated (ITO/PEDOT:PSS/P3HT:PCBM/ZnO/Al) as shown in Figure S3. The active area is 0.06 cm2, which is about 1000 times large than the photodetector devices fabricated in this work. By comparison of the on-current per unit area at 0 V, the device with the asymmetrical RGO-Ti electrodes shows a slightly higher current density than that based on the sandwich structure, which can be attributed to the less light absorption and reflection in the former device structure.

Table S1. Comparison of the on/off ratio of the P3HT and P3HT:PCBM blend photodiodes based on the coplanar asymmetrical and symmetrical electrodes.

Electrodes	Materials	On/off		Photoresponse speed
		0 V	0.4 V	
Asymmetrical electrodes	P3HT	> 1000	~ 3	fast
	P3HT:PCBM	> 1000	~ 50	fast
Symmetrical electrodes	P3HT	—	~1.2*	slow
	P3HT:PCBM	—	~(10-10000)**	fast

The on/off ratios of the photodetectors based on the asymmetrical electrodes are calculated from Figure 3.

* The value is calculated from Figure 4(b) with the gap length of 5 um. Similar results have also been obtained based on symmetrical gold (or graphene) electrodes with ~ 100 nm gap length.[10, 27]

** The on/off ratio highly depends on the gap length. High on/off ratio (~10000) can be obtained when the gap length is in the range of 75 — 100 nm.[27] Typically, on/off ratio decreases sharply to ~ 10 when the gap length increases to 5 um (Figure 4d).